Macromolecules
ARTICLE

Macromolecules **2010**, *43*, 4379–4383 **4379**
DOI: 10.1021/ma9028344

Measurement of Phase Transition Free Energies in Polyelectrolyte−Surfactant Complexes

Michael Leonard[‡] and Helmut H. Strey*[,†]

[†]*Biomedical Engineering Department, Stony Brook University, Stony Brook, New York 11794-2580, and* [‡]*Polymer Science and Engineering Department, University of Massachusetts Amherst, Amherst, Massachusetts 10003*

Received December 26, 2009; Revised Manuscript Received March 28, 2010

ABSTRACT: When polyelectrolytes are mixed with oppositely charged surfactants at a 1:1 charge ratio, long-range ordered polyelectrolyte−surfactant complexes are formed. In this paper we demonstrate that by using the "Luzzati method" combined with osmotic stress measurements, we were able to determine the polyelectrolyte−surfactant free energy change while transitioning from a *Pm*3*n* cubic phase to a hexagonal phase. Assuming that the major contribution to this energy originates from bending energies associated with the structural rearrangements of the surfactants, we determined the bending modulus of the surfactant inside the complex.

Luzzati and Husson[1] were the first to demonstrate that controlled hydration of condensed lipid bilayers, in conjunction with X-ray scattering, provided a reasonable estimate of the average lipid area in these systems. Since then, many others have used this method to explore the energetics of self-assembled soft matter systems.[2−10] In this work, we demonstrate the measurement of the free energy associated with the *Pm*3*n* ↔ hcpc transition of polyelectrolyte−surfactant complexes[11−15] by combining the osmotic stress[16] and controlled hydration methods.[1] Even though phase diagrams of polyelectrolyte−surfactant systems are by now well established, we are the first to measure free energy of transitions in these systems. For this demonstration, we have focused on the 70% charge PAAm−CTACl system in 100 mM NaCl because it exhibited a rather narrow cubic−hexagonal coexistence region.[13]

Figure 1 shows the structure of both phases. The structure of the *Pm*3*n* in self-assembled amphiphilic systems has caused much discussion in the literature.[17] It is now commonly believed that the *Pm*3*n* structure is formed by disconnected micellar aggregates. Figure 1 shows the model by Fontell et al.[18] in which two types of elongated micelles (two of one kind and six of the other kind) pack into the unit cell. The hexagonal phase consists of infinitely long cylindrical micelles with the polyelectrolyte in between.

Poly(acrylate-*co*-acrylamide) (PAAm, Polysciences, 70% carboxylate content, M_n = 200 000 g mol^{-1}, sodium chloride (Mallinckrodt), cetyltrimethylammonium chloride (CTACl, Aldrich, 1.04 M aqueous solution), poly(ethylene glycol) (PEG, Fluka, M_n = 8000 g mol^{-1}), and ethylenediaminetetraacetic acid (EDTA, Sigma molecular biology grade) were used as received. Tris(hydroxymethylaminomethane) (TRIS base, Sigma molecular biology grade) was adjusted to pH 7.0 (HCl) before use. Concentrated solutions of PAAm (5 wt %) were prepared in 100 mM NaCl and were buffered in a mixture of 10 mM TRIS base/1 mM EDTA (10-1 TE). All aqueous solutions were prepared using water purified via reverse osmosis.

PAAm−CTACl complexes for use in the hydration experiments were prepared by combining 1.04 M CTACl solution with a stoichiometric amount (based on charge) of 5 wt % PAAm solution, followed by vigorous mixing. Immediately upon the addition of ∼10 mL of water to these mixtures, a fine white precipitate formed. The precipitate was isolated by centrifugation, washed with three 50 mL aliquots of water to remove excess ions, and allowed to air-dry for ∼8 h. Pieces of the air-dried complexes were then vacuum-dried at room temperature for ∼12 h. Small amounts of the vacuum-dried complexes were quickly massed and placed in polyethylene Eppendorf tubes. Known amounts of 100 mM NaCl were added to each dehydrated sample such that a water-per-surfactant range of 8−28 was covered. After adding the appropriate amounts of NaCl solution to the dehydrated complexes, the Eppendorf tubes were sealed and were subsequently allowed to equilibrate for 3 weeks. After this time, all of the added salt solution appeared to have fully penetrated the complexes such that each sample was qualitatively homogeneous.

The osmotic stress experiments were conducted in the following way. Pieces of dried complexes were placed in large reservoirs of aqueous 100 mM NaCl with PEG concentrations in each solution ranging from 30 to 41 wt %, corresponding to an approximate osmotic pressure range of 20−55 atm.[19] The samples were then allowed to equilibrate with the stressing solutions for 1 month at room temperature. During this time, samples were periodically vortexed to ensure PEG solution homogeneity during the dehydration process.

Small-angle X-ray scattering (SAXS) measurements were performed with a Rigaku RU-H3R rotating anode X-ray diffractometer operating at 1.2 kW. The diffractometer was equipped with a multilayer focusing optic (point focus = 100 μm^2; Osmic Inc., type CMF23-46Cu8) and a custom-built evacuated Statton-type scattering camera. The sample cells used for both the Luzzati and solution osmotic stress measurements consisted of a Teflon card sandwiched between thin Mylar windows that allowed the solid samples to remain in equilibrium with the stressing solutions during the measurements while isolating the samples from vacuum. The transfer of each sample from its equilibrated environment to the sample holder was performed as quickly as possible, so as to minimize exposure to the external environment. Because of the small increments of water content and osmotic pressure

*To whom correspondence should be addressed.

Published on Web 04/09/2010

required for this study, several replicate samples were analyzed for each experiment to establish reasonable statistics. The sample-to-detector distance was 460 mm, which corresponds to a q range of 0.0698 Å^{-1} ≤ q ≤ 0.625 Å^{-1} with $q = (4\pi/\lambda)\sin(\theta/2)$, where θ is twice the Bragg angle, and the incident beam wavelength was 1.54 Å, corresponding to 8 keV Cu Kα radiation. Scattering patterns were acquired with 10 cm × 15 cm Fuji ST-VA image plates in conjunction with a Fuji BAS-2500 image plate scanner. The scattering intensity profiles were obtained from radial averages of the scattering pattern intensities, using procedures developed by our research group for the Igor Pro software package (Wavemetrics, Inc., Lake Oswego, OR).

The controlled hydration of PAAm−CTACl complexes resulted in a transition from a distinct hcpc phase to a *Pm3n* phase via a two-phase coexistence region, as shown in Figure 2. These results were highly correlated with the osmotic stress results, as shown by the selected SAXS profiles from the osmotic stress experiments in Figure 3. The hcpc and *Pm3n* unit cell sizes derived from the replicate SAXS measurements are shown in Tables 1 and 2; note that the data obtained from both methods were quite precise and that the coexistence region was successfully bracketed by both methods. The unit cell volumes of the *Pm3n* ($V \sim a^3$) and hcpc ($V \sim a^2$) structures increased linearly with increasing water content as shown in Figure 3. This result confirms that the volume change accompanying the *Pm3n* ↔ hcpc transition can indeed be attributed to the change in water content.

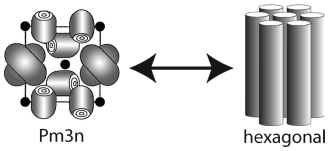

Figure 1. Phase transition between *Pm3n* cubic phase and a hexagonal phase in a polyelectrolyte−surfactant complex. The model for the *Pm3n* phase is adapted from ref 18 in which two types of elongated micelles (two of one and six of the other type) are packed in the unit cell.

Phase diagrams derived from the osmotic pressure and hydration experiments are presented in Figures 4 and 5. Because we have characterized the *Pm3n* ↔ hcpc phase transition as a function of both osmotic pressure and the change in water volume, we now have the basis for determining the free energy. The transition pressure was explicitly determined by using the relative intensities of the hcpc phase from the SAXS traces shown in Figure 2. These values were plotted in Figure 4a versus osmotic pressure and were fit to a sigmoid curve. The inflection point of this curve, which was calculated during the fitting procedure, was interpreted as the transition point. From Figure 3, we find that $\Pi = 3.89 \times 10^7$ dyn cm^{-2} at the midpoint of the coexistence region, representing the transition pressure. Since three water molecules comprise the width of the coexistence region (Figure 5), the associated volume change was 3 H_2O × 30 Å^3 = 90 Å^3; we assume that this volume change occurs at a constant transition pressure. Therefore, the free energy of the *Pm3n* ↔ hcpc transition was calculated as

$$\frac{\Delta F}{N} = (3.89 \times 10^6\ \mathrm{N/m^2})(9 \times 10^{-29}\ \mathrm{m^3}) = 3.50 \times 10^{-22}\ \mathrm{J}$$

which is equivalent to 0.088 k_BT per surfactant molecule. This value is significant because it represents the energetic cost of removing water from the cubic phase to form the hexagonal phase. The fact that the free energy change is small relative to k_BT helps to explain why we have often observed coexisting *Pm3n* and

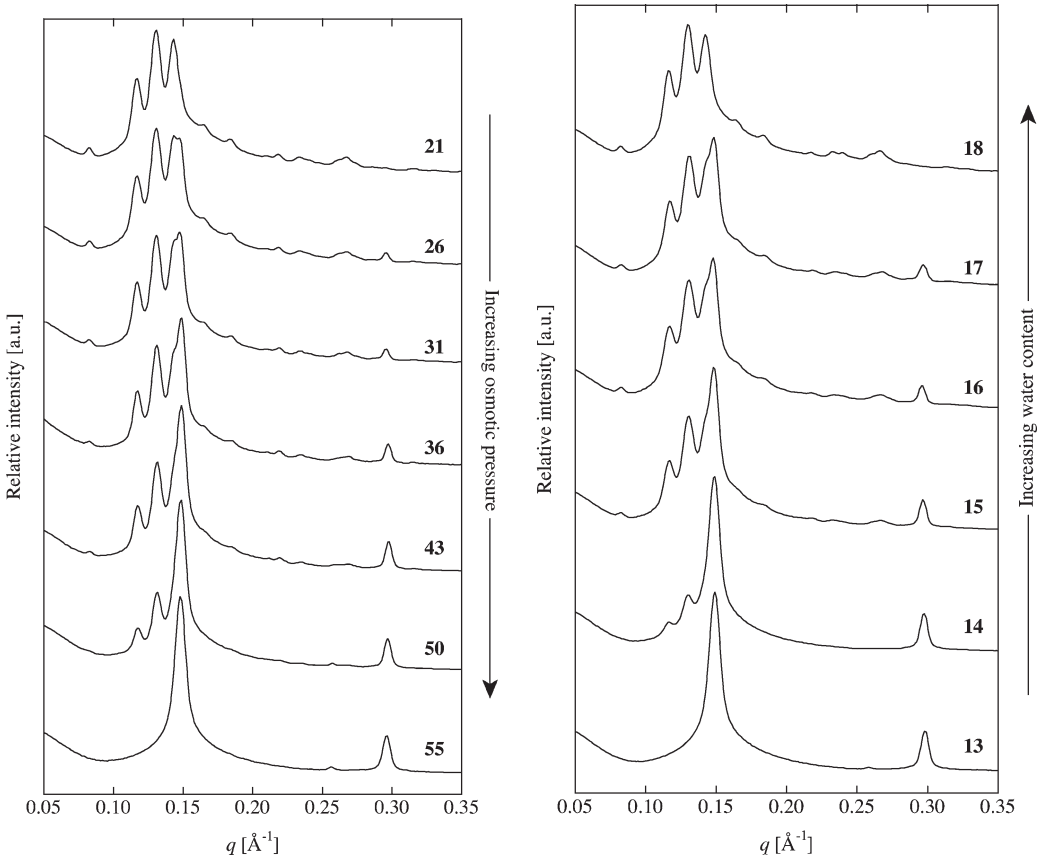

Figure 2. Angular-averaged SAXS profiles for 70% charge PAAm−CTACl complexes at 100 mM ionic strength, showing the evolution of the hcpc phase from the *Pm3n* phase with increasing osmotic pressure (left) and increasing water content (right). Each curve represents the average of *at least four* replicate measurements.

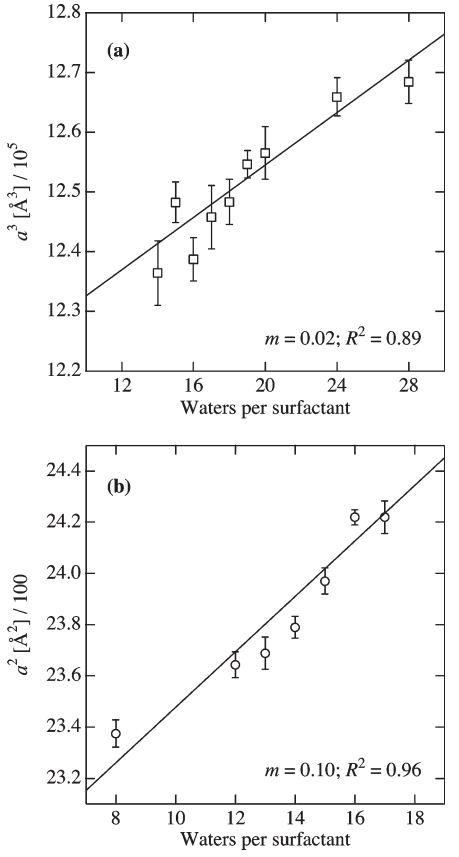

Figure 3. Unit cell volume versus water content for (a) *Pm*3*n* and (b) hcpc systems. Volume axes have been scaled by the indicated factors for more convenient presentation. Linear regression parameters are shown for each plot.

Table 1. Structural Data from Replicate Hydration Experiments

		hcpc			*Pm*3*n*		
n_w/surfactant	N	d_B [Å]	a [Å]	RSD [%]	d_B [Å]	a [Å]	RSD [%]
8	9	41.87	48.35	0.13	—[a]	—	—
12	9	42.11	48.62	0.12	—	—	—
13	5	42.15	48.67	0.15	—	—	—
14	5	42.24	48.77	0.10	48.00	107.33	0.25
15	8	42.40	48.96	0.12	48.15	107.67	0.16
16	9	42.62	49.21	0.07	48.03	107.40	0.17
17	9	42.62	49.21	0.15	48.12	107.60	0.25
18	9	—	—	—	48.15	107.67	0.18
19	9	—	—	—	48.23	107.85	0.11
20	9	—	—	—	48.26	107.91	0.20
24	9	—	—	—	48.38	108.18	0.15
28	9	—	—	—	48.41	108.25	0.16

[a] No structure observed.

hcpc phases in the PAAm−CTAX system; these two structures are very energetically similar and can be interconverted by thermal energy. For perspective, consider that the magnitude of this result is quite similar to the water binding energy determined for partially disordered, gel-phase dimyristoylphosphatidylcholine bilayers.[3]

As we alluded to earlier, the energetic cost of removing water from the PAAm−CTACl complex can be largely attributed to the bending of its constituent surfactant monolayers as the *Pm*3*n* phase is converted to the hcpc phase. It would therefore be useful to have an estimate of the bending stiffness of these amphiphilic aggregates at the transition point. The measured free energy change ($\Delta F = F_{hcpc} - F_{Pm3n}$) can be attributed to a change in the monolayer curvature according to eq 1. We assume that the *Pm*3*n*

Table 2. Structural Data from Replicate Osmotic Stress Experiments

		hcpc			*Pm*3*n*		
log[Π (dyn cm^{-2})]	N	d_B [Å]	a [Å]	RSD [%]	d_B [Å]	a [Å]	RSD [%]
7.34	6	—[a]	—	—	48.11	107.58	0.12
7.38	4	—	—	—	48.12	107.60	0.09
7.42	5	42.51	49.08	0.04	48.04	107.43	0.13
7.45	5	42.48	49.05	0.02	48.01	107.35	0.09
7.49	4	42.47	49.04	0.03	48.00	107.33	0.08
7.53	4	42.46	49.03	0.04	47.93	107.16	0.07
7.57	4	42.33	48.88	0.05	47.93	107.17	0.14
7.60	5	42.30	48.84	0.07	47.91	107.12	0.05
7.64	4	42.22	48.75	0.01	47.90	107.12	0.01
7.67	4	42.21	48.74	0.03	47.79	106.86	0.11
7.71	5	42.18	48.71	0.15	47.81	106.91	0.13
7.74	6	42.17	48.69	0.16	—	—	—

[a] No structure observed.

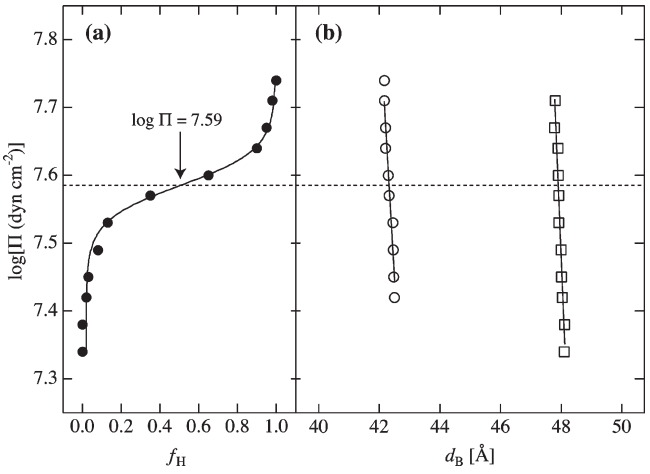

Figure 4. (a) Increase of the hcpc phase fraction (f_H) with increasing osmotic pressure, as determined from relative SAXS intensities. The inflection point of the sigmoid fitting function was interpreted as the transition pressure (dashed line). (b) Phase diagram for PAAm−CTACl complexes at 100 mM ionic strength. Bragg spacings were calculated using the (100) hcpc (○) and the (210) *Pm*3*n* cubic (□) diffraction signals when those phases were present.

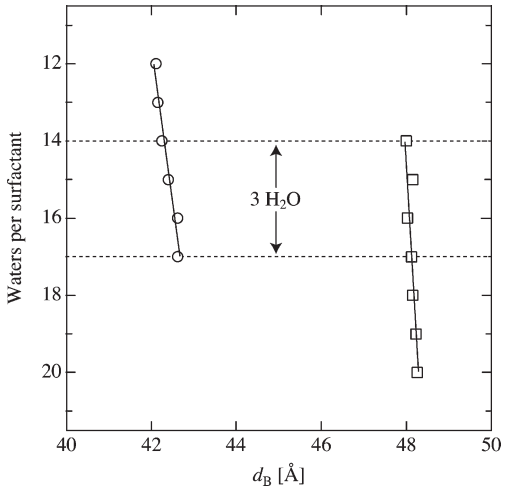

Figure 5. Water content versus Bragg spacing for PAAm−CTACl complexes at 100 mM ionic strength. Bragg spacings were calculated using the (100) hcpc (○) and the (210) *Pm*3*n* cubic (□) diffraction signals when those phases were present. The width of the coexistence region was used to calculate the volume change associated with the transition, which was assumed to occur at constant osmotic pressure.

phase includes mostly spherical aggregates such that

$$F_{Pm3n} = \int \mathrm{d}A \left[\frac{1}{2}K\left(\frac{1}{R_1}+\frac{1}{R_1}+\frac{2}{R_0}\right)^2\right] \quad (1)$$

For the hcpc phase, the free energy can be written in a similar fashion:

$$F_{\mathrm{hcpc}} = \int \mathrm{d}A \left[\frac{1}{2}K\left(\frac{1}{R_2}-\frac{2}{R_0}\right)^2\right] \quad (2)$$

We further assume that the radii of the surfactant aggregates are equal to the spontaneous radius of curvature throughout the phase transition such that $R_1 = R_2 = R_0$. Therefore, $F_{Pm3n} = 0$ and $\Delta F = F_{\mathrm{hcpc}}$. On a per-surfactant basis, the free energy change can be written as follows:

$$\frac{\Delta F}{N} = \frac{A_{\mathrm{cyl}}}{N_{\mathrm{cyl}}}\left(\frac{1}{2}K\frac{1}{{R_0}^2}\right) = \frac{2\pi R_2 L}{N_{\mathrm{cyl}}(L)}\left(\frac{1}{2}K\frac{1}{{R_0}^2}\right) \quad (3)$$

We can write $N_{\mathrm{cyl}}(L)/L$ in terms of the density, $\rho = N/V$, which we assume remains constant throughout the phase transition:

$$\frac{N_{\mathrm{cyl}}(L)}{L} = \frac{\rho V_{\mathrm{cyl}}}{L} \quad (4)$$

Since $V_{\mathrm{cyl}} = \pi R^2 L$, eq 3 can then be rewritten as

$$\frac{\Delta F}{N} = \frac{2}{\rho R_2}\left(\frac{1}{2}K\frac{1}{{R_0}^2}\right) \quad (5)$$

Again, we assume that the densities of the spherical and cylindrical phases are identical such that $\rho = 3N/4\pi {R_0}^3$. Substituting ρ into eq 5 yields our working expression for the free energy in terms of the bending stiffness, K:

$$\frac{\Delta F}{N} = \frac{4\pi {R_2}^2}{N}\left(\frac{1}{3}K\frac{1}{{R_0}^2}\right) = \frac{1}{3}K\frac{A}{N}\frac{1}{{R_0}^2} \quad (6)$$

In this expression, A/N is the area per surfactant molecule in a spherical aggregate. Roelants has shown that the aggregation number for CTACl micelles can vary widely as ionic strength is varied:[20] For example, N was shown to increase from 136 to 176 as ionic strength was increased from 104 to 155 mM. Using those data as a starting point, we assume that the aggregation number for surfactant moieties within a polyelectrolyte−surfactant complex will be larger than that of the analogous pure surfactant system due to additional screening from the polyelectrolyte. For this analysis, we estimated that the aggregation number for surfactant moieties in the PAAm−CTACl system was in the range of 150−200. Once the aggregation number is known, R_0 can then be estimated from[20]

$$R_0 = \left[\frac{3N(V_{\mathrm{H}}+V_{\mathrm{C}})}{4\pi}\right]^{1/3} \quad (7)$$

where V_{H} and V_{C} are the surfactant headgroup and hydrophobic tail volumes, respectively. For CTACl, Roelants[20] found that $V_{\mathrm{H}} = 170$ Å^3 and $V_{\mathrm{C}} = 458$ Å^3. Thus, R_0 was calculated to be 28.2 and 31.1 Å for aggregation numbers of 150 and 200, respectively. Substituting these values into eq 6 along with $\Delta F/N$, we estimate the bending modulus K to span a range of 3.2−4.2 $k_{\mathrm{B}}T$. We note that the magnitude of this value is very similar those obtained from surfactant systems with similar chain lengths.[21−23] However, we cannot make a direct comparison of our result to the bending moduli of other polyelectrolyte−surfactant systems; these values are difficult to measure, and in this context, we are not aware of any previously reported work.

The thermodynamically well-defined conditions under which osmotic stress experiments are carried out strictly prohibit phase coexistence at equilibrium. It is interesting, then, to consider how the magnitude of $\Delta F/N$ might relate to the unexpected presence of cubic−hexagonal coexistence regions in the PAAm−CTACl phase diagram. If the *Pm3n* and hcpc phases can be interconverted by thermal energy at room temperature, then the energy required to transform at least one CTACl micelle into a cylinder should be on the order of $k_{\mathrm{B}}T$. However, the results presented here indicate that the transition energy is much larger than $k_{\mathrm{B}}T$. Using our measured value of $\Delta F/N$ (0.088 $k_{\mathrm{B}}T$) and a conservative estimate of the micellar aggregation number for CTACl (150), we estimate the total free energy to be roughly 13 $k_{\mathrm{B}}T$. Clearly, this value is too large to explain the phase coexistence we have observed. As such, the complexes studied here have likely not reached their true equilibrium states, possibly due to large kinetic barriers that may be associated with the transition.

The cubic-to-hexagonal phase transition in polyelectrolyte−surfactant complexes exemplifies the geometrically frustrated competition between spontaneous curvature and molecular packing constraints. Using a combination of osmotic stress and controlled hydration experiments, the energetic cost of removing water from the *Pm3n* cubic phase to form the hcpc phase in the PAAm−CTACl system at 100 mM ionic strength was found to be 0.088 $k_{\mathrm{B}}T$ per surfactant at room temperature. Under these conditions, the bending stiffness of the surfactant monolayers within the complex was estimated to be in the range of 3−4 $k_{\mathrm{B}}T$, which is consummate with values obtained for nonionic surfactant−oil−water microemulsions with similar surfactant chain lengths.

Acknowledgment. H.H.S. was supported by the Office of Basic Energy Sciences, Materials Sciences and Engineering Division, of the U.S. Department of Energy under Grant ER46323. We also acknowledge support from the National Science Foundation through the University of Massachusetts Amherst Materials Research Science and Engineering Center (DMR-0213695).

References and Notes

(1) Luzzati, V.; Husson, F. *J. Cell Biol.* **1962**, *12* (2), 207–216.
(2) Gruner, S. M.; Parsegian, V. A.; Rand, R. P. *Faraday Discuss.* **1986**, *81*, 29–37.
(3) Hung, W. C.; Chen, F. Y. *Chin. J. Phys.* **2000**, *38* (4), 882–892.
(4) Hung, W. C.; Chen, F. Y. *Chin. J. Phys.* **2003**, *41* (1), 85–91.
(5) Rand, R. P.; Fuller, N. L.; Gruner, S. M.; Parsegian, V. A. *Biochemistry* **1990**, *29* (1), 76–87.
(6) Chen, F. Y.; Hung, W. C.; Huang, H. W. *Phys. Rev. Lett.* **1997**, *79* (20), 4026–4029.
(7) Gawrisch, K.; Parsegian, V. A.; Hajduk, D. A.; Tate, M. W.; Gruner, S. M.; Fuller, N. L.; Rand, R. P. *Biochemistry* **1992**, *31*, 2856–2864.
(8) Costigan, S. C.; Booth, P.; Templer, R. H. *Mol. Cryst. Liq. Cryst.* **2000**, *352*, 59–66.
(9) Seddon, J. M.; Robins, J.; Gulik-Krzywicki, T.; Delacroix, H. *Phys. Chem. Chem. Phys.* **2000**, *2*, 4485–4493.
(10) Smith, G. S.; Sirota, E. B.; Safinya, C. R.; Clark, N. A. *Phys. Rev. Lett.* **1988**, *60* (9), 813–816.
(11) Antonietti, M.; Burger, C.; Effing, J. *Adv. Mater.* **1995**, *7* (8), 751–753.
(12) Ilekti, P.; Piculell, L.; Tournilhac, F.; Cabane, B. *J. Phys. Chem. B* **1998**, *102*, 344–351.
(13) Leonard, M. J.; Strey, H. H. *Macromolecules* **2003**, *36* (25), 9549–9558.
(14) Zhou, S.; Hu, H.; Burger, C.; Chu, B. *Macromolecules* **2001**, *34*, 1772–1778.
(15) Berret, J. F.; Vigolo, B.; Eng, R.; Herve, P.; Grillo, I.; Yang, L. *Macromolecules* **2004**, *37* (13), 4922–4930.

(16) Parsegian, V. A.; Rand, R. P.; Fuller, N. L.; Rau, D. C. Osmotic Stress for the Direct Measurement of Intermolecular Forces. In *Methods in Enzymology*; Packer, L., Ed.; Academic Press: New York, 1986; Vol. *127*, pp 400−416.
(17) Seddon, J. M.; Templer, R. H. *Philos. Trans. R. Soc. London, Ser. A* **1993**, *344* (1672), 377–401.
(18) Fontell, K.; Fox, K. K.; Hansson, E. *Mol. Cryst. Liq. Cryst.* **1985**, *1* (1−2), 9–17.
(19) Stanley, C. B.; Strey, H. H. *Macromolecules* **2003**, *36* (18), 6888–6893.
(20) Roelants, E.; De Schryver, F. C. *Langmuir* **1987**, *3* (2), 209–214.
(21) Castro-Roman, F.; Porte, G.; Ligoure, C. *Langmuir* **2001**, *17* (16), 5045–5058.
(22) Jung, H.-T.; Lee, S. Y.; Kaler, E. W.; Coldren, B.; Zasadzinski, J. A. *Proc. Natl. Acad. Sci. U.S.A.* **2002**, *99* (24), 15318−15322.
(23) Safinya, C. R.; Roux, D.; Smith, G. S.; Sinha, S. K.; Dimon, P.; Clark, N. A.; Bellocq, A. M. *Phys. Rev. Lett.* **1986**, *57* (21), 2718–2721.